MICROFABRICATED ATOMIC CLOCKS

J. Kitching[1], S. Knappe[1], L. Liew[2], P. Schwindt[1], V. Shah[3], J. Moreland[2] and L. Hollberg[1]
[1]Time and Frequency Division, NIST, Boulder, CO, USA
[2]Electromagnetics Division, NIST, Boulder, CO, USA
[3]Department of Physics, The University of Colorado, Boulder, CO, USA

ABSTRACT

We summarize the development of microfabricated atomic frequency references at NIST. The physics packages of these devices have volumes near 10 mm^3 and power dissipation below 150 mW, and can potentially achieve a fractional frequency instability in the range of 10^{-11} over long periods. A fully integrated frequency reference could find application in portable, battery-operated devices such as global positioning system (GPS) receivers and cellular telephones.

1. INTRODUCTION

For over fifty years, clocks based on electromagnetic oscillations of atoms have provided the most precise method of timing events lasting longer than a few minutes. So precise are these "atomic" clocks, that in 1967 the second was redefined to be the time taken for a Cs atom in a particular quantum state to undergo exactly 9,192,631,770 oscillations. More recently, atomic clocks have found application in a variety of critical infrastructures and scientific experiments that require highly precise timing. These include synchronization of communication networks [1], global positioning [2], long-baseline interferometry [3] and even tests of fundamental theories in physics such as Einstein's theory of relativity [4].

While the long-term precision of atomic clocks is unsurpassed, the size and power required to run these devices has prevented their use in a variety of areas, particularly in those applications requiring portability or battery operation. The NIST F-1 primary standard, for example, occupies an entire table and requires many hundreds of watts to operate. The state of the art in compact commercial atomic frequency references are Rb vapor-cell devices with volumes near 100 cm^3 that operate on a few watts of power and cost about $1000.

Miniaturization based on microelectromechanical systems (MEMS) offers many of the same compelling advantages to atomic frequency references as it does to other large-scale technologies. In addition to small size, a corresponding improvement in the device power dissipation is gained because the heat lost to the environment via the device surface is smaller. MEMS also could enable high-volume, wafer-based production of atomic clocks, which would substantially reduce cost. Such improvements would make atomic timekeeping useful in a variety of advanced applications where quartz clocks are now used.

One example is a jam-resistant global positioning system (GPS) receiver for the military. Because of the extremely low power of the signal broadcast by GPS satellites, receivers are highly susceptible to intentional jamming and unintentional interference from other RF sources transmitting in the same frequency band. Because of the larger bandwidth over which the military P(Y) signal is transmitted, it is considerably less susceptible to jamming than the civilian C/A signal. However, since the P(Y) code repeats only every seven days, a P(Y) receiver needs a better local clock than in a C/A receiver in order to narrow down its search window and reduce the time required to find the code match [5,6]. Existing P(Y) receivers usually have to first lock onto the civilian C/A signal, which eliminates the anti-jam advantage of the larger-bandwidth P(Y) signal. If the receiver's local clock were capable of determining the time to within 1 ms over several days, it would be possible for a receiver to lock onto the P(Y) signal directly without first acquiring the C/A signal. Thus, the receiver would be significantly more resistant to jamming.

The frequency-reference physics package developed at NIST [7] is the first atom-based reference to present significant potential for battery operation. In addition, its small size and amenability to wafer-level fabrication and assembly make it appealing for commercialization and integration into other devices. Hence, chip-scale atomic clocks (CSACs) based on physics packages such as these open the door to the application of atomically precise timing in a wide range of portable, battery operated devices.

2. ATOMIC FREQUENCY REFERENCES

Most atomic clocks are passive devices, in which the atoms serve as the basic frequency reference but do not oscillate on their own. In these devices, the atomic oscillation is excited by applying an electromagnetic field from a secondary oscillator, usually based on a quartz crystal resonator. By comparing the frequency of the applied field to the resonant frequency of the atomic oscillation, the applied field can be locked to the atomic frequency. This is an output frequency that is highly stable over weeks or months of operation.

The frequency reference therefore comprises three main functional components. The physics package is the heart of the clock and contains the atomic vapor cell that determines the clock output frequency. The physics package takes as its input an oscillating microwave signal, whose frequency is possibly quite unstable, generated by the second component, the local oscillator (LO). The output of the physics package is a voltage proportional to the difference between the frequency of the LO and the resonant frequency of the atoms. The third component of the clock is a control system, which stabilizes the LO frequency to the atomic resonance and also performs certain

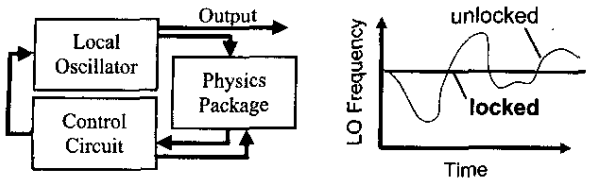

Figure 1: Functional diagram of a passive atomic frequency reference.

other tasks such as stabilizing the temperature of the atomic vapor cell to reduce temperature-induced changes in the atomic resonance frequency. An optional fourth component, a frequency divider can phase-coherently divide the stabilized LO frequency from the range of 1 to 10 GHz typical of atomic resonance frequencies down to near 10 MHz, which is useful for many applications. A diagram outlining the main functional components is shown in Figure 1.

The most recent work at NIST has focused on the development of the physics package. Previously, the smallest atomic-clock physics packages have been based on alkali vapor cells fabricated using traditional glass-blowing techniques and have had volumes of roughly 1 cm^3 [8]. In addition, the power required to run the physics package has been quite high (near 1 W), partly because of the need to heat the large cell to its operating temperature of a few tens of degrees Kelvin above ambient. Finally, the physics packages are expensive to fabricate in a commercial setting since components must be manufactured and assembled individually into complete devices. The microfabrication approach developed by NIST and others in the DARPA-CSAC program is potentially able to simultaneously address all of these issues and enable the fabrication of small, low-power and inexpensive physics packages for use in new generations of compact atomic clocks.

3. ATOMIC EXCITATION SCHEME

In most vapor-cell atomic clocks, the atomic resonance is excited with a microwave field applied directly to the atomic sample. In this case the orientation of the magnetic moment of the orbital electron is altered with respect to the orientation of the nuclear magnetic moment. Typically, the atomic vapor cell is placed in a microwave cavity resonant with the radiation needed to excite the transition, which confines the microwave radiation in the vicinity of the atomic sample. While this excitation scheme works very well in large-scale atomic clocks, a difficulty presents itself when shrinking the size of the physics package to below the wavelength of the excitation microwave field since in this regime, a traditional empty cavity will not be resonant.

A compelling alternative is to excite the atomic resonance with two optical fields, separated in frequency by that of the atomic resonance. Because of the nonlinearity in the response of the atom to optical fields, oscillation at the difference frequency can be generated in the atom without ever actually applying a field at this frequency directly to the atom. A phenomenon called coherent population trapping (CPT) [9] allows the simultaneous excitation of the atomic oscillation and monitoring of the atomic response through the optical power absorbed by the atoms.

In practice, CPT is implemented through the modulation of the injection current of a diode laser. Since the frequency of the light emitted by the laser depends on the injection current, sidebands are created on the optical carrier by this modulation process. If the laser is modulated at one-half the atomic resonance frequency, the two first-order sidebands can become the two optical fields needed for the CPT effect. As little as 100 μW of RF power is required to achieve a modulation index of near unity. The atomic resonant response is observed by scanning the laser modulation frequency around the atomic resonance frequency and detecting the power of the light transmitted through the cell. This implementation is illustrated in Figure 2.

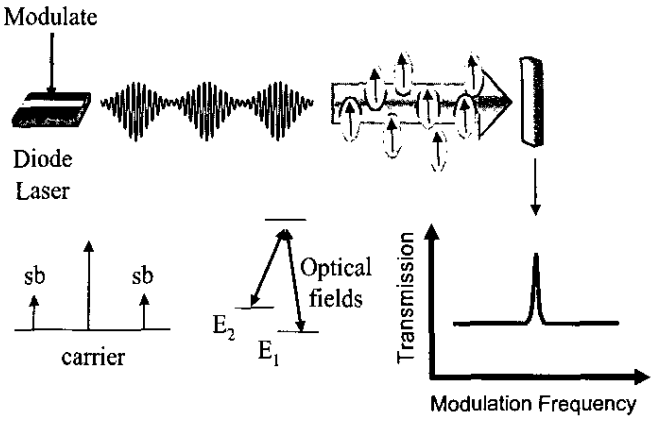

Figure 2: Coherent population trapping excitation and observation of the atomic oscillation.

4. ATOMIC CELL FABRICATION

The heart of the atomic clock physics package is a vapor cell containing a combination of alkali atoms, and a buffer gas to reduce the wall-induced decoherence of the hyperfine oscillation. Vapor cells have traditionally been fabricated using conventional glass-blowing techniques, which have two important drawbacks. Firstly, it is difficult to make very small cells because of the increasing importance of surface tension in shaping the melted glass at small sizes. Secondly, the cells must be made individually, leading to substantial fabrication cost and difficulty integrating the cells with other clock components.

We have developed a method of cell fabrication [10,11] based on techniques usually applied to MEMS. The cells are formed by sandwiching an etched Si wafer between two transparent glass wafers, as shown in Figure 3. A Si wafer, typically a few hundred micrometers thick (Figure 3a), is lithographically patterned and etched by use of wet-chemical (KOH) or deep-reactive-ion etching. By use of one of these processes, holes are etched through the wafer with a square

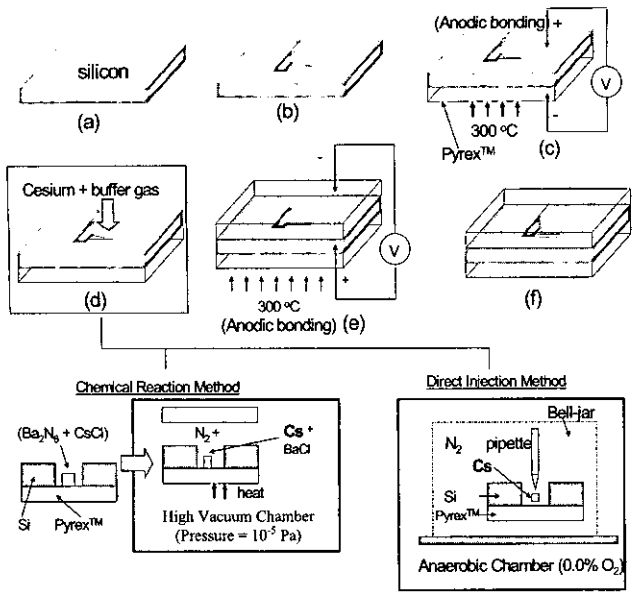

Figure 3: Schematic showing the steps in wafer-level fabrication of an alkali cell.

cross-section of sides roughly 0.6 mm (Figure 3b). However, the highly scalable nature of the etching process would allow holes as small as a few tens of micrometers to be created simply by changing the etch mask.

Once the holes are created in the Si wafer, glass is attached to one side using the technique of anodic (or field-assisted) bonding [12]. This process can be used to bond flat wafers of borosilicate glass to a variety of materials including other glasses, metals and Si. The bonding process is carried out by placing the two clean wafers in contact in a dust-free environment. The sample is then heated to approximately 300 °C and a few hundred volts of potential difference is applied across the wafer pair (Figure 3c). Because of the high temperature, impurity ions in the glass (such as K^+ and Na^+) begin to drift in the electric field, leaving behind electrons. The electrons form a space-charge field, which attracts one material to the other and creates a strong bond between them. The bond is fully hermetic and ideal for confining alkali atoms inside the cell, as far as we have been able to ascertain.

Once the initial piece of glass is bonded onto one side of the Si wafer (Figure 3c), Cs (or Rb) is then deposited into the cell (Figure 3d and subpanels). This is carried out with one of two methods. The first method involves the chemical reaction of BaN_6 and CsCl in a high-vacuum environment. These two materials are both soluble in water and are deposited into the cell preform in solution. The water is then evaporated and the preform, with remaining chemicals in solid form, is placed into a high-vacuum chamber. The chamber is evacuated and backfilled with a buffer gas at an appropriate pressure. The sample is then heated to 150 °C, at which point the chemicals react and create Cs, BaCl and N_2. A second glass piece is then pushed up against the top of the sample, and the cell is heated further with an electric field applied to seal the Cs and buffer gas inside the cell (Figure 3e). The residual N_2 gas produced by the reaction presumably is pumped or diffuses away before the cell is sealed, since the final buffer-gas pressure in the cell roughly matches the pressure in the chamber during bonding.

The second technique of cell filling involves the use of an anaerobic chamber, essentially an airtight glove box with the water and oxygen reacted away. The cell preform is placed in the anaerobic chamber and Cs is added by breaking open a Cs ampoule inside the chamber and injecting some of the liquid metal using a micropipette. The cell preform is then placed inside a bell jar (inside the anaerobic chamber) that is backfilled with the desired buffer gas. The second window is then attached, again by use of anodic bonding.

After the final bonding step, the cells can be diced into individual components (Figure 3f). A cell fabricated using the first method described above is shown in Figure 4. We believe that the process outlined in Figure 3 could be easily implemented at the wafer level. Lithographic patterning, etching and bonding of entire wafers are routinely done in the MEMS field, and cell filling could be carried out either with an automated Cs dispenser (anaerobic chamber technique) or simultaneous deposition of chemical solution (chemical reaction technique).

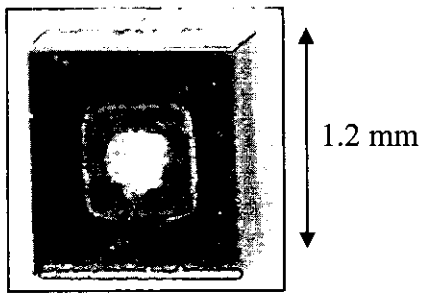

Figure 4: Photograph of a micromachined Cs vapor cell fabricated by anodic bonding.

5. PHYSICS PACKAGE ASSEMBLY

A schematic and photographs of a fully integrated physics package are shown in Figure 5. A die containing a vertical-cavity surface-emitting laser (VCSEL) is bonded onto a substrate patterned with gold (Figure 5A, layer a). The VCSEL is used because of its low power requirements (typically < 5 mW for most devices), high modulation efficiency, and availability of single-mode devices at the 852 nm optical transition in Cs and the 795 nm optical transition in Rb.

The light emitted by the VCSEL is conditioned by an optics assembly (Figure 5A, layers b-f) attached to the baseplate. This optics assembly attenuates and collimates the light and changes the light polarization from linear to circular. In this vertically integrated structure, glass spacers (Figure 5A, layer b) support the rest of the clock assembly over the laser and provide thermal isolation between the heated cell and the baseplate. Two neutral-density filters (Figure 5A, layers c and f), cut from a wafer of optically dense glass, attenuate the light power to roughly 10 μW, and the light is collimated using a

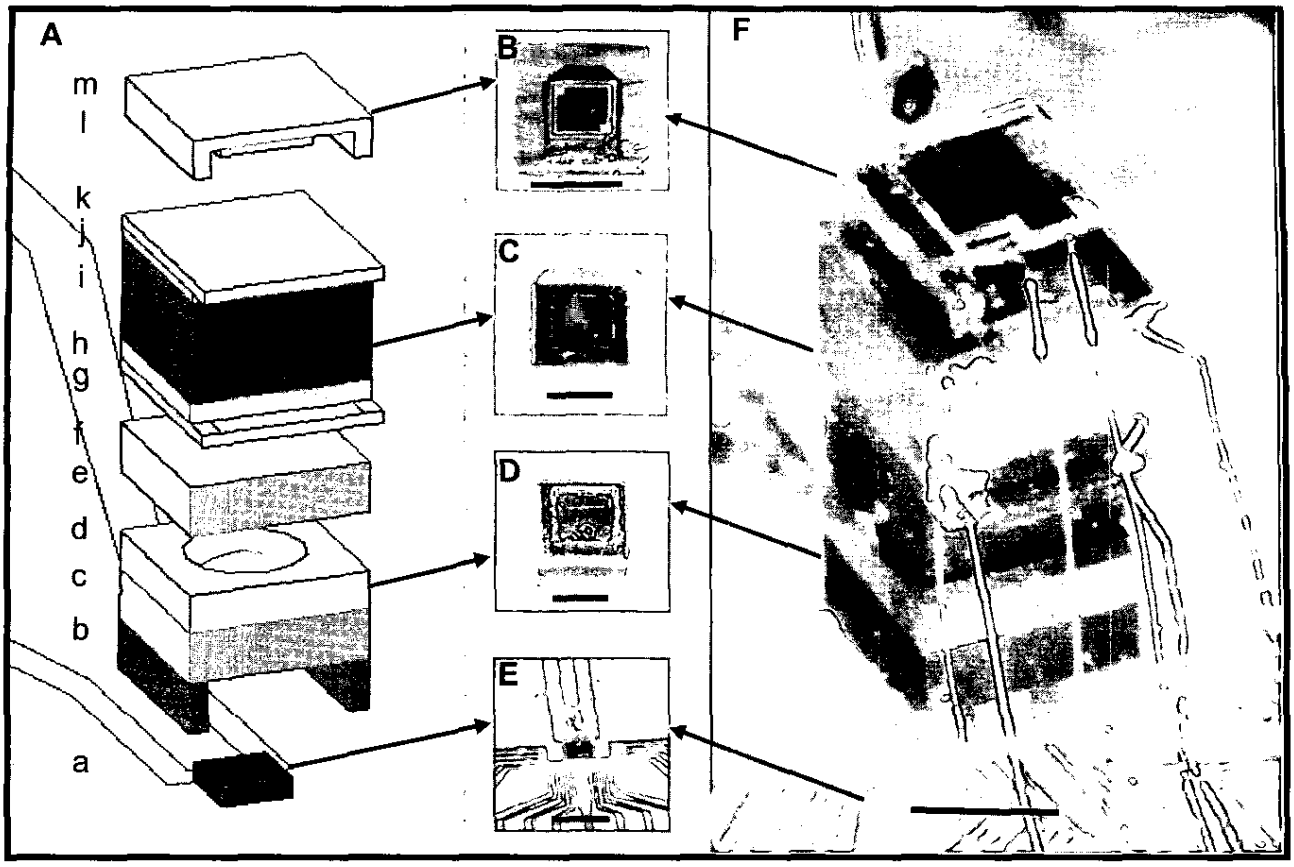

Figure 5: The microfabricated atomic clock physics package based on Cs atoms. (A) Schematic of assembly. Layers from bottom to top: a, Laser and baseplate; b, Glass (500 μm); c, ND filter (500 μm); d, Spacer (375 μm); e, Quartz (70 μm, not shown); f, ND filter (500 μm); g, Glass/ITO (125 μm/30 nm); h, Glass (200 μm); i, Si (1000 μm); j, Glass (200 μm); k, Glass/ITO (125 μm/30 nm); l, Si (375 μm); m, Glass (125μm). Total height, 4.2 mm, width and depth, 1.5 mm. Photographs (B), photodiode assembly, (C), cell assembly, (D), optics assembly and (E), laser assembly and (F), the full atomic clock physics package realized as a microchip. The black lines in the photographs indicate 1 mm.

commercially available micro-refractive lens fabricated by inkjet deposition of optical epoxy (Figure 5A, layer d). The light polarization is altered with a piece of a quartz wafer, 80 μm thick, with its optical axis oriented at 45° to the direction of the initial polarization of the laser beam (Figure 5A, layer e, not shown).

The cell assembly (Figure 5A, layers g-k) is placed on top of the optics assembly. During operation of the clock, the cell is heated with planar heaters (Figure 5A, layers g and k), fabricated from a thin layer of transparent indium-tin oxide (ITO) deposited on a glass substrate and then wire-bonded to the substrate through gold contact strips. Heaters are placed above and below the cell to provide uniform heating when a current is passed through the ITO film. Because the heat enters the cell though the windows, these parts remain slightly warmer than the cell body, which prevents buildup of a opaque alkali metal film on the windows that might prevent light from entering or exiting the cell.

Finally a photodiode assembly (Figure 5A, layers l-m) is mounted onto the top of the structure to detect the light power transmitted through the cell.

In most cases, the layers are bonded together with optical epoxy. Gold wires of thickness 25 μm are bonded on one end to individual components before they are assembled and the other end is bonded to the baseplate after assembly. We anticipate that with further refinement of the design, all wire-bonding can be done after assembly of the entire structure. Photographs of the fully assembled device and individual components are shown in Figure 5B-F.

6. DEVICE CHARACTERIZATION

The physics package is operated by first heating the alkali vapor cell to about 80 °C. At this temperature, vapor-phase Cs atoms are in equilibrium with the liquid phase at a density of about 10^{13} atoms/cm^3, which is sufficient for observation of the atomic resonance. Modulation at 4.6 GHz, one-half of the Cs ground-state hyperfine oscillation frequency, is applied to the laser. As the modulation frequency is swept around the

frequency of the atomic resonance, a change in the DC optical power transmitted through the cell occurs, which is detected with the photodiode at the top of the structure. A plot of the photodiode signal as a function of the detuning of twice the modulation signal is shown in Figure 6. The resonance width of 7.1 kHz gives a Q-factor of 1.2×10^{6}.

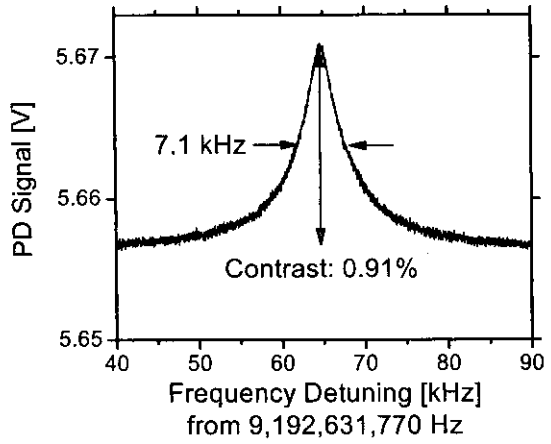

Figure 6: Atomic resonance signal from the microfabricated atomic clock physics package shown in Figure 5.

By modulating the frequency of the local oscillator and using lock-in detection, an error signal can be generated from the resonance in Figure 6. When this error signal is fed back to the frequency-tuning port of the LO, the LO frequency can be stabilized onto the atomic resonance. The stabilized output frequency of the LO is then compared to a secondary, more stable oscillator to measure its frequency as a function of time; a plot of these data is shown in Figure 7. When integrated for a time τ, the fractional frequency instability as measured by the Allan deviation is shown in Figure 8. An instability of 2.5×10^{-10} at one second of integration is obtained, which integrates down to a minimum of 4×10^{-11} near 100 s. A linear drift of -1.6×10^{-8}/day is also observed, which we attribute to chemical reactions occurring in the cell that change the pressure of the buffer gas and therefore also the frequency of the clock. It is expected that this drift can be reduced substantially by fabricating cells that do not contain Ba. Although the direct injection method of cell filling shown in Figure 3 does not involve Ba, cells made with this method have not yet been tested with regard to long-term frequency stability.

The short-term instability of the frequency reference is determined by the resonance width (Q-factor) and the noise present at the photodetector. The resonance width is dominated in this particular clock by optical power-broadening, with secondary contributions due to collisions of alkali atoms with the walls of the cell and buffer-gas atoms. The noise is dominated by shot-noise in the conversion of optical power into electrons in the photodiode.

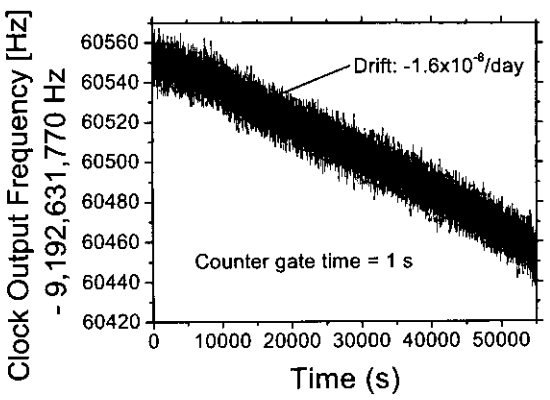

Figure 7: Output frequency of the microfabricated atomic clock as a function of time.

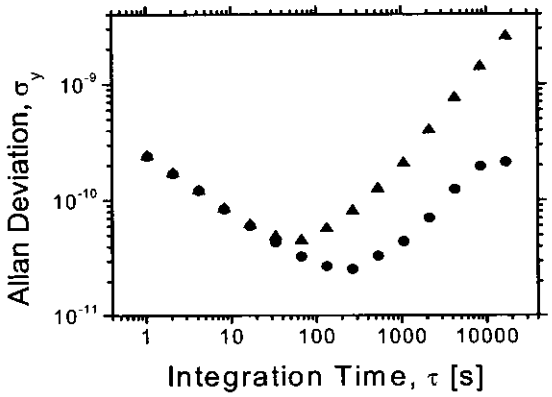

Figure 8: Fractional frequency instability of the microfabricated atomic frequency reference as a function of integration time. Triangles indicate the stability as-measured and circles indicate the stability after removal of the linear frequency drift.

7. POWER DISSIPATION

The electrical power required to run the physics package was 71 mW, and was dominated by the power required to heat the cell above the ambient temperature of 46 °C set by the baseplate. The high baseplate temperature was required to tune the particular laser used in the device to the correct wavelength and is not generally necessary; the frequency reference was in fact operated without baseplate heating but the short-term instability was somewhat higher. An advantage obtained through the use of a VCSEL is the extremely low power (< 2 mW) required to both run the laser and to modulate it with amplitude sufficient to excite the CPT resonance.

By modeling the heat flow in the structure, both analytically and with a finite-element computation, the heat loss channels could be roughly identified, as shown in Figure

9. We estimate that 30 mW is lost through the lower spacer unit, and that 24 mW is lost through the six gold wire bonds providing the electrical connections to the baseplate. The remainder is presumably lost through radiation and through conduction to the air surrounding the physics package. Our modeling suggests that these last two heat-loss channels could be reduced to well below one milliwatt by use of vacuum packaging with a low-emissivity coating on its interior surface. The remaining sources of heat loss, conduction through the lower spacer unit and the wire-bonds, can be addressed through more advanced thermal design of the spacer unit itself. For example, the use of a polymer material with a lower thermal conductivity and thin (10 μm) gold traces as part of the electrical path would reduce the heater power to below 12 mW to maintain a temperature difference of 50 K between the baseplate and the cell.

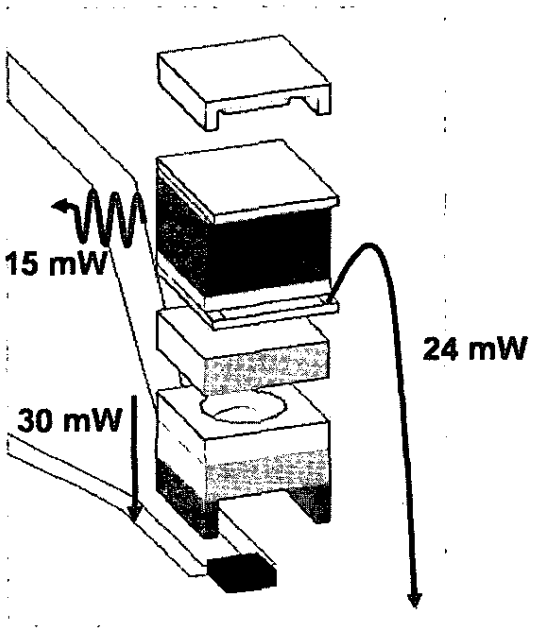

Figure 9: Estimated heat-loss channels in an early chip-scale atomic clock.

8. INTEGRATED SYSTEM

As mentioned above, two other components are required, in addition to the physics package, to form a complete atomic frequency reference. The development of small low-power oscillators at GHz-frequencies with sufficient frequency stability to be able to be locked to the atomic resonance is being undertaken by a number of research groups. In addition, a digital control system based on a microprocessor is being developed at NIST and is expected to be able to implement the four feedback loops necessary to run the clock. The anticipated power budget of the complete frequency reference is outlined in Table 1.

Table 1. Anticipated power budget for fully integrated chip-scale atomic clock.

Component	Power	Confidence
Heating of cell (modeling)	11.1 mW	high
Laser DC power (measured)	4 mW	high
Laser RF power (measured)	70 μW	high
Local oscillator (estimate)	8.6 mW	low
Control circuit (estimate)	4.5 mW	moderate
B-field, temp. sensor, etc.	< 1 mW	high
Total:	**29.3 mW**	**moderate**

9. OTHER APPLICATIONS

While the main goal of our research over the last two years has been to design and build highly miniaturized atomic clocks, the basic technologies developed as part of this research program have significant applications in other areas. One example is highly sensitive and accurate magnetometers [13] based on vapors of alkali atoms. Because atoms have a magnetic moment, different orientations of certain atomic states in an external magnetic field have different internal energies. Since the energy difference is proportional to the magnetic field (at least at low field strengths), measuring this energy difference is equivalent to measuring the strength of the magnetic field. It is therefore possible to determine the magnetic field by comparing the energy difference of magnetically sensitive states to the energy difference of magnetically insensitive states (or some other stable frequency), as shown in Figure 10.

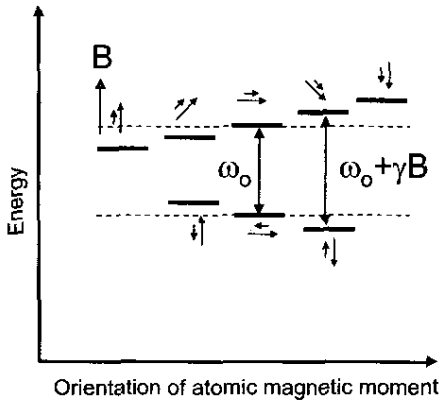

Figure 10: A magnetometer based on the orientation of atomic (nuclear and electronic) magnetic moments in a magnetic field.

Operationally, this can be accomplished by simply tuning the frequency of the local oscillator in a chip-scale atomic clock from the magnetically insensitive transition at ω_0 to a magnetically sensitive one at $\omega_0+\gamma B$, where B is the magnitude of the external magnetic field and γ is a constant. This change in LO frequency causes an oscillation between two atomic states whose energy depends on magnetic field. A magnetometer of this type has been implemented at NIST [14] with a microfabricated structure similar to that in Figure 5 but based on ^{87}Rb atoms, rather than Cs. With this device

magnetic fields can be measured with a sensitivity of $40\,pT/\sqrt{Hz}$ in the frequency range of 10 Hz to 100 Hz. The output of the device when subject to an external magnetic field stepped by 2.53 nT every ten seconds is shown in Figure 11.

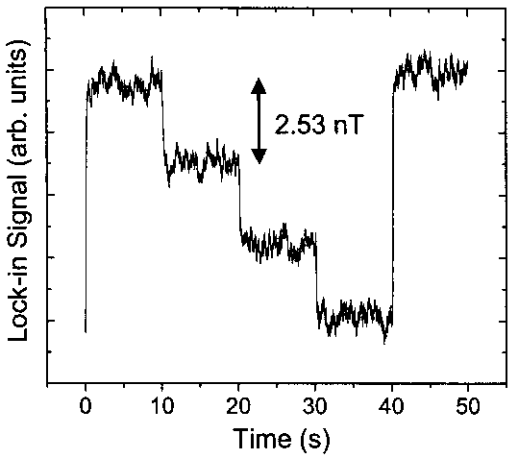

Figure 11: The magnetometer output signal is plotted as a function of time as the magnetic flux is stepped in 10-second intervals. The averaging time is 30 ms.

10. CONCLUSION

The convergence of the two fields of MEMS and atomic physics has generated a number of important research opportunities in recent years. Spectacular recent results in developing integrated atom optics systems using MEMS and laser cooling [15], for example, may some day result in accelerometers and gyroscopes that perform orders of magnitude better that what can be done today.

The field of precision timing is also now experiencing the revolutionary impact MEMS has had in a wide range of other areas, from chemical detection to power sources. It seems likely that atomic clocks based on MEMS fabrication techniques will become commercial products in the near future. Commercialization will undoubtedly result in significant improvements in design and performance, leading to smaller, lower-power and less costly devices. In turn, new applications will emerge that are not even on the horizon today. The work described in this paper represents just the first few tentative steps in this direction and many important challenges remain to be overcome. But the profound impact technologies such as highly miniaturized atomic clocks and magnetometers may have in a variety of basic infrastructures will almost certainly drive MEMS implementations of these devices forward rapidly toward a future that is bright. And small.

This work is funded by NIST and the Microsystems Technology Office of the Defense Advanced Research Projects Agency (DARPA). This work is a contribution of NIST, an agency of the US Government, and is not subject to copyright.

REFERENCES

[1] J. A. Kusters and C.A. Adams, "Performance requirements of communication base station time standards," *RF Design*, vol. 22, pp. 28-38, 1999.

[2] B. W. Parkinson and J. J. Spilker, Jr., eds., "Global positioning system: theory and applications," *Prog. Astronautics Aeronautics,* vol. 163, 1996.

[3] K. I. Kellermann and A. R. Thompson, "The very long baseline array," *Science*, vol. 229, pp. 123-130, 1985.

[4] R.V.C. Vessot, et al., "Test of relativistic gravition using a space-borne hydrogen maser," *Phys. Rev. Lett.*, vol. 45, pp. 2081-2084, 1980.

[5] H. Fruehoff, "Fast "direct-P(Y)" GPS signal acquisition using a special portable clock," *Proc. 33rd Ann. Precise Time and Time Interval (PTTI) Meeting*, Long Beach, Nov. 27-29, 2001, pp. 359-369.

[6] R. L. Filler and R. D. Esposti, "Clock performance and direct GPS P(Y)-code (re)acquisition," *Proc. IEEE Int. Freq. Control Symp.*, Pasadena, May 27-29, 1998, pp. 315-319.

[7] S. Knappe, L. Liew, V. Shah, P. Schwindt, J. Moreland, L. Hollberg, and J. Kitching, "A micromachined atomic clock," *Appl. Phys. Lett.* vol. 85, pp. 1460-1462, 2004.

[8] P.J. Chantry, I. Liberman, W.R. Verbanets, C. F. Petronio, R. L. Cather, and W. D. Partlow, "Miniature laser-pumped cesium cell atomic clock oscillator," *Proc. IEEE Int. Frequency Control Symp.*, Honolulu, June 5-7, 1996, pp. 1002-1010.

[9] E. Arimondo, "Coherent population trapping in laser spectroscopy," *Progress in Optics*, vol. 35, pp. 257-354, 1996.

[10] L. Liew, S. Knappe, J. Moreland, H. G. Robinson, L. Hollberg and J. Kitching, "Micromachinined alkali atom vapor cells," *Appl. Phys. Lett.* vol. 84, pp. 2694-2696, 2004.

[11] L-A. Liew, S. Knappe, J. Moreland, H. Robinson, L. Hollberg and J. Kitching, "Micromachined alkali atom vapor cells for chip-scale atomic clocks," *Proc. IEEE Int. Conf. Micro Elect. Mech. Syst.* Maastricht, Jan. 25-29, 2004, pp. 113-116.

[12] G. Wallis and D. I. Pomerantz, "Field assisted glass-metal sealing," *J. Appl. Phys.* vol. 40, pp. 3946-3949, 1969.

[13] H. Dehmelt, "Modulation of a light beam by precessing absorbing atoms," *Phys. Rev.*, vol. 105, pp. 1924-1925, 1957.

[14] P. D. D. Schwindt, S. Knappe, V. Shah, L. Hollberg, J. Kitching, L. Liew and J. Moreland, "A chip-scale atomic magnetometer," *Appl. Phys. Lett.*, in press.

[15] D. Z. Anderson, V. M. Bright, L. Czaia, S. Du, S. Frader-Thompson, B. McCarthy and M. Squires, "Atom optics on a chip," *Proc. IEEE Int. Conf. Micro Elect. Mech. Syst.*, Kyoto, Jan 19-23, 2003, pp. 210-214.